DE87001393

www.NTIS.gov
One Source. One Search. One Solution.

NOVEL FISCHER-TROPSCH SLURRY CATALYSTS AND PROCESS CONCEPTS FOR SELECTIVE TRANSPORTATION FUEL PRODUCTION. QUARTERLY TECHNICAL PROGRESS REPORT, 1 APRIL-30 JUNE 1985

AIR PRODUCTS AND CHEMICALS, INC.
ALLENTOWN, PA

JUL 1986

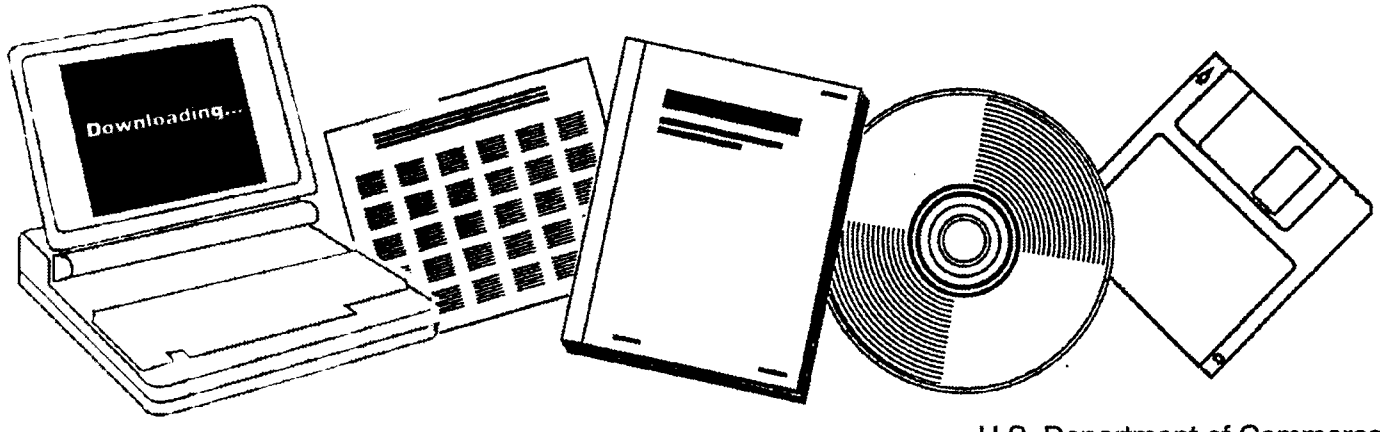

U.S. Department of Commerce
National Technical Information Service

One Source. One Search. One Solution.

NTIS

Providing Permanent, Easy Access to U.S. Government Information

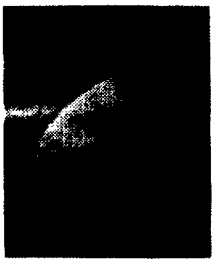

National Technical Information Service is the nation's largest repository and disseminator of government-initiated scientific, technical, engineering, and related business information. The NTIS collection includes almost 3,000,000 information products in a variety of formats: electronic download, online access, CD-ROM, magnetic tape, diskette, multimedia, microfiche and paper.

Search the NTIS Database from 1990 forward

NTIS has upgraded its bibliographic database system and has made all entries since 1990 searchable on **www.ntis.gov.** You now have access to information on more than 600,000 government research information products from this web site.

Link to Full Text Documents at Government Web Sites

Because many Government agencies have their most recent reports available on their own web site, we have added links directly to these reports. When available, you will see a link on the right side of the bibliographic screen.

Download Publications (1997 - Present)

NTIS can now provides the full text of reports as downloadable PDF files. This means that when an agency stops maintaining a report on the web, NTIS will offer a downloadable version. There is a nominal fee for each download for most publications.

For more information visit our website:

www.ntis.gov

U.S. DEPARTMENT OF COMMERCE
Technology Administration
National Technical Information Service
Springfield, VA 22161

DOE/PC/70030--T3

DE87 001393

AIR PRODUCTS

NOVEL FISCHER-TROPSCH SLURRY CATALYSTS AND PROCESS CONCEPTS FOR SELECTIVE TRANSPORTATION FUEL PRODUCTION

QUARTERLY TECHNICAL PROGRESS REPORT

FOR THE PERIOD 1 APRIL - 30 JUNE 1985

W. EAMON CARROLL

NELLIE CILEN

STEPHEN A. MOTIKA

HOWARD P. WITHERS, JR.

AIR PRODUCTS AND CHEMICALS, INC.

ALLENTOWN, PA 18105

Patent Cleared - CH 12/4/86

PREPARED FOR UNITED STATES DEPARTMENT OF ENERGY

UNDER CONTRACT NO. DE-AC22-84PC70030

MASTER

DISTRIBUTION OF THIS DOCUMENT IS UNLIMITED

AIR PRODUCTS

DISCLAIMER

This report was prepared as an account of work sponsored by the United States Government. Neither the United States nor the United States Department of Energy, nor any of their employees, makes any warranty, express or implied, or assumes any legal liability or responsibility for the accuracy, completeness, or usefulness of any information, apparatus, product, or process disclosed, or represents that its use would not infringe privately owned rights. Reference herein to any specific commercial product, process, or service by trade name, mark, manufacturer, or otherwise, does not necessarily constitute or imply its endorsement, recommendation, or favoring by the United States Government or any agency thereof. The views and opinions of authors expressed herein do not necessarily state or reflect those of the United States Government or any agency thereof.

AIR PRODUCTS

PATENT HOLD

This documented copy, since it is transmitted in advance of patent clearance, is made available in confidence solely for the use in performance of work under contracts with the United States Department of Energy. This document is not to be published nor its contents otherwise disseminated or used for purposes other than specified above before patent approval for such release or use has been secured, upon request from the Chief, Office of Patent Counsel, United States Department of Energy, 9800 South Cass Avenue, Argonne, Illinois 60439.

- CONTAINS POTENTIALLY PATENTABLE DATA — NOT FOR PUBLICATION ->

EXECUTIVE SUMMARY

In the third quarter of the Air Products and Chemicals, Inc./United States Department of Energy contract, "Novel Fischer-Tropsch Slurry Catalysts and Process Concepts for Selective Transportation Fuel Production", work continued on the two major tasks: Task 2 — Development of Improved Supported Catalyst Compositions and Task 3 — Slurry Reactor Kinetic Studies. Within Task 2, work was accomplished in studying the effect of catalyst activation procedure on activity and selectivity of the basecase $Co_2(CO)_8/Zr(OPr)_4/Al_2O_3$ composition. Activation with pure H_2 gave a > 100% increase in both bulk and specific activity in gas phase tests at 220°C compared to the standard syngas activation. However, the activity enhancement was somewhat less at higher run temperatures. To establish a reference for the cobalt carbonyl-based catalysts, a catalyst was prepared and gas phase tested in which cobalt nitrate was used as the cobalt source and supported on zirconated alumina. Syngas and pure H_2 activation were also compared for this catalyst. A $Co_2(CO)_8/Zr(OPr)_4/Al_2O_3$ catalyst with increased cobalt loading was prepared to examine the effect of metal loading on catalyst performance. Initial analysis of these catalysts has been carried out using X-ray photoelectron spectroscopy (XPS) and H_2 chemisorption. Four catalysts were screened in the slurry phase reactors. These included the titanium promoted $Co_2(CO)_8$ on alumina catalyst, the $Co_2(CO)_8/Zr(OPr)_4$ on alumina composition having a higher Co/Zr weight ratio of 1.15, and the potassium promoted mixed-metal composition of $FeCo_3(CO)_{12}$ on alumina. The fourth slurry screening test was done to examine the effect of pure H_2 activation on the performance of the basecase $Co_2(CO)_8/Zr(OPr)_4$ on alumina catalyst.

Task 2 — Development of Improved Supported Catalyst Compositions

The performance of cobalt carbonyl-based catalysts was never directly compared to that of catalysts prepared from more conventional, non-carbonyl cobalt sources. To determine this reference point, a catalyst was prepared using cobalt nitrate on zirconated alumina with the

same metals loading as the cobalt carbonyl basecase. Gas phase testing using the standard syngas activation showed that it was 30% less active than the carbonyl derived catalyst. Selectivity was also changed with the nitrate derived catalyst giving a more even distribution of hydrocarbon products such that larger amounts of both methane and wax were produced. The $Co(NO_3)_2/Zr/Al_2O_3$ catalyst was also gas phase tested using a pure H_2 activation. This procedure resulted in better performance such that identical specific activity to the syngas-activated catalyst was achieved with the H_2-activated catalyst at 23°C lower temperature. The carbonyl-derived catalyst activated with syngas, however, was still slightly more active at similar run conditions. Hydrogen activation of the nitrate-based catalyst resulted in a hydrocarbon selectivity more like the carbonyl-based catalyst, but with higher wax selectivity. Thus, cobalt carbonyl provides a catalyst having greater activity and better liquid fuel selectivity than conventional cobalt salts.

A large batch (366 g) of the basecase $Co_2(CO)_8/Zr(OPr)_4/Al_2O_3$ composition was prepared by the standard procedure in order to compare the standard syngas activition with pure H_2 activition in gas phase tests. Hydrogen activation again provided an increase in activity. At 220°C, both bulk and specific activity increased by greater than 100%. At 240°C, the increase of 27% was not as great and at 260°C activities were similar for both activations. There was no obvious effect on hydrocarbon selectivity in these gas phase tests. It should be noted that in comparative studies like this the slurry reactor will give more meaningful results due to better control of process conditions.

To study the effect of higher cobalt metal loading on catalyst performance, a large batch of $Co_2(CO)_8/Zr(OPr)_4/Al_2O_3$ catalyst was prepared having a Co loading of 10.8% and Co/Zr ratio of 1.3. Since it has been shown that the Co/Zr ratio is not highly critical, the Co/Zr ratio was increased to facilitate the preparation of such a highly loaded support. This has not yet been tested.

- CONTAINS POTENTIALLY PATENTABLE DATA — NOT FOR PUBLICATION -

XPS data have been obtained on the basecase $Co_2(CO)_8/Zr(OPr)_4/Al_2O_3$ catalyst, both as freshly prepared and after H_2 activation, as well as on the $Co(NO_3)_2$-derived catalyst in the oxidized form. For the carbonyl-based catalyst, the data indicate the presence of only oxidized cobalt in both fresh and activated samples. This suggests the formation of difficult to reduce cobalt aluminates and zirconates or at least a strong interaction between Co and the support. Hydrogen chemisorption data for both the basecase and higher loading $Co_2(CO)_8/Zr(OPr)_4/Al_2O_3$ catalyst show cobalt metal surface areas of 6 m^2/g or less and cobalt dispersions of 10% or less. This agrees with the XPS data indicating only small amounts of reduced cobalt.

Four catalysts were screened in the 1 liter slurry phase reactors this quarter. The results are summarized here. For the following three catalysts, the standard synthesis gas activation method was used:

- A $Co_2(CO)_8/Al_2O_3$ catalyst promoted with titanium rather than zirconium. During the initial test conditions at 240°C, the best activity and selectivity for liquid fuels, C_5-C_{23}, was observed. No improvement was noticeable upon raising the temperature to 260°C and then to 280°C. Compared with the basecase catalyst, this catalyst was less active, but was superior in liquid fuels selectivity, which accounted for 60 wt% of the total hydrocarbons. Testing at 600 psig proved to be detrimental to both the activity and selectivity of this catalyst. This confirmed prior observations about the Co-based catalysts. Future screening of cobalt catalysts will be confined to pressures below 300 psig.

- A variation on the metal to promoter weight ratio of the $Co_2(CO)_8/Zr(OPr)_4$ on alumina catalyst, Co/Zr = 1.15, compared with the standard 0.56. As with the titanium-promoted catalyst, the maximum selectivity of liquid fuels was obtained at the lowest temperature tested, 240°C, and the lowest CO/H_2 feed gas ratios, where selectivities of 67-70 wt% were observed. The activity of this catalyst was poor; comparable to the unpromoted $Co_2(CO)_8/Al_2O_3$ catalyst (run #7887-67-445),

but lower than that of the basecase catalyst having the 0.56 Co/Zr ratio. Figure 1 illustrates the differences in specific activity observed versus Co/Zr wt ratio at 240°C and 260°C for the three loading variations tested to date.

- An $FeCo_3(CO)_{12}$ cluster on alumina catalyst promoted with potassium. The activity of this catalyst was similar to that of the basecase $Co/Zr/Al_2O_3$ catalyst, giving similar bulk and specific activities. Liquid fuels selectivity was better than that of the basecase catalyst. At 240°C and 260°C, the C_5-C_{23} selectivity was 70 wt% but dropped to 60 wt% at 280°C. Although this catalyst contained iron, the water-gas shift activity was no better than the basecase catalyst.

A fourth catalyst, $Co_2(CO)_8$ on zirconated alumina, with approximately the standard Co/Zr weight ratio of 0.65, was activated using pure H_2 for comparison.

- A substantial improvement in both activity and selectivity was observed. Initially, at 220°C, CO/H_2 = 1.0 and 1.85 NL/g cat/hr, the bulk activity was nearly double that of the $Co_2(CO)_8/Zr(OPr)_4/Al_2O_3$ catalyst activated with synthesis gas. At higher temperatures, 240°C - 280°C, the difference was not as pronounced, but still apparent with a 15% improvement. Overall, at the higher CO/H_2 ratio of 2.0 and reduced space velocity of 0.95 NL/g cat/hr, the rate of synthesis gas conversion was independent of temperature. The selectivity pattern showed a greater dependence on temperature than on the CO partial pressure. The liquid fuels selectivity was substantial at over 70 wt% at 260°C; this is 20% higher than the results using synthesis gas activation.

Task 3 — Slurry Reactor Kinetic Studies

Part of this task was addressed this quarter by examining the mechanistic concepts involving olefin reincorporation. These experiments were performed by adding 10 to 20 volume percent ethylene to the feed gas

during the slurry test of the $Co_2(CO)_8/Zr(OPr)_4/Al_2O_3$ catalyst (run # 7888-33-73i, Co/Zr = 1.15). Hydrogenation of ethylene to ethane was the major reaction. There was little change observed in the hydrocarbon selectivity. The selectivity to oxygenates, however, increased from 0.2 to 2.0 wt%, but with strictly propanol production. Propanol accounted for 10 wt% of the oxygenate fraction compared to less than 1.0 wt% when no ethylene was added to the feed.

TABLE OF CONTENTS

		PAGE
1.0	INTRODUCTION	1
2.0	OBJECTIVE	3
3.0	RESULTS AND DISCUSSION	5
	3.1 Task 1 — Project Work Plan	5
	3.2 Task 2 — Development of Improved Supported Catalyst Compositions	5
	(a) Catalyst Preparation	5
	(b) Gas Phase Screening	7
	(c) Slurry Reactor Tests	10
	(d) Catalyst Characterization	23
	3.3 Task 3 — Slurry Reactor Kinetic Studies	25
4.0	EXPERIMENTAL	27
	4.1 Task 2 — Development of Improved Supported Catalyst Compositions	27
	(a) Catalyst Preparation	27
	(b) Gas Phase Tests	29
	(c) Slurry Reactor Tests	29
	(d) Catalyst Characterization	31
5.0	ACKNOWLEDGEMENTS	32

- CONTAINS POTENTIALLY PATENTABLE DATA — NOT FOR PUBLICATION -

LIST OF TABLES

TABLE		PAGE
1	Summary of Gas Phase Tests	33
2	Comparative Catalyst Test Data — Slurry Tests	35
3	Slurry Screening Summary, $Co_2(CO)_8/Ti(OPr)_4/Al_2O_3$ — 7888-1-589	36
	$Co_2(CO)_8/Ti(OPr)_4/Al_2O_3$ Mass Balance Results — 7888-1-589	
4	Mass Balance Process Conditions and Product Summary — Sample 4	37
5	Hydrocarbon Distribution — Sample 4	38
6	Mass Balance Process Conditions and Product Summary — Sample 6	40
7	Hydrocarbon Distribution — Sample 6	41
8	Mass Balance Process Conditions and Product Summary — Sample 9	43
9	Hydrocarbon Distribution — Sample 9	44
10	Mass Balance Process Conditions and Product Summary — Sample 12	46
11	Hydrocarbon Distribution — Sample 12	47
12	Mass Balance Process Conditions and Product Summary — Sample 15	49
13	Hydrocarbon Distribution — Sample 15	50
14	Mass Balance Process Conditions and Product Summary — Sample 17	52
15	Hydrocarbon Distribution — Sample 17	53
16	Mass Balance Process Conditions and Product Summary — Sample 20	55
17	Hydrocarbon Distribution — Sample 20	56
18	Mass Balance Process Conditions and Product Summary — Sample 22	58

19	Hydrocarbon Distribution — Sample 22	59
20	Mass Balance Process Conditions and Product Summary — Sample 24	61
21	Hydrocarbon Distribution — Sample 24	62
22	Mass Balance Process Conditions and Product Summary — Sample 26	64
23	Hydrocarbon Distribution — Sample 26	65
24	Mass Balance Process Conditions and Product Summary — Sample 31	67
25	Hydrocarbon Distribution — Sample 31	68
26	Mass Balance Process Conditions and Product Summary — Sample 33	70
27	Hydrocarbon Distribution — Sample 33	71
28	Mass Balance Process Conditions and Product Summary — Sample 35	73
29	Hydrocarbon Distribution — Sample 35	74
30	Mass Balance Process Conditions and Product Summary — Sample 37	76
31	Hydrocarbon Distribution — Sample 37	77
32	Mass Balance Process Conditions and Product Summary — Sample 41	79
33	Hydrocarbon Distribution — Sample 41	80
34	Slurry Screening Summary, $Co_2(CO)_8/Zr(OPr)_4/Al_2O_3$ — 7888-33-731	82
	$Co_2(CO)_8/Zr(OPr)_4/Al_2O_3$ Mass Balance Results — 7888-33-731	
35	Mass Balance Process Conditions and Product Summary — Sample 8	83
36	Hydrocarbon Distribution — Sample 8	84
37	Mass Balance Process Conditions and Product Summary — Sample 10	86
38	Hydrocarbon Distribution — Sample 10	87
39	Mass Balance Process Conditions and Product Summary —	89

	Sample 12	
40	Hydrocarbon Distribution — Sample 12	90
41	Mass Balance Process Conditions and Product Summary — Sample 16	92
42	Hydrocarbon Distribution — Sample 16	93
43	Mass Balance Process Conditions and Product Summary — Sample 21	95
44	Hydrocarbon Distribution — Sample 21	96
45	Mass Balance Process Conditions and Product Summary — Sample 24	98
46	Hydrocarbon Distribution — Sample 24	99
47	Mass Balance Process Conditions and Product Summary — Sample 28	101
48	Hydrocarbon Distribution — Sample 28	102
49	Mass Balance Process Conditions and Product Summary — Sample 33	104
50	Hydrocarbon Distribution — Sample 33	105
51	Mass Balance Process Conditions and Product Summary — Sample 36	107
52	Hydrocarbon Distribution — Sample 36	108
53	Mass Balance Process Conditions and Product Summary — Sample 37	110
54	Hydrocarbon Distribution — Sample 37	111
55	Mass Balance Process Conditions and Product Summary — Sample 44	113
56	Hydrocarbon Distribution — Sample 44	114
57	Mass Balance Process Conditions and Product Summary — Sample 47	116
58	Hydrocarbon Distribution — Sample 47	117
59	Mass Balance Process Conditions and Product Summary — Sample 52	119
60	Hydrocarbon Distribution — Sample 52	120
61	Mass Balance Process Conditions and Product Summary — Sample 56	122

62	Mass Balance Process Conditions and Product Summary — Sample 59	123
63	Mass Balance Process Conditions and Product Summary — Sample 62	124
64	Mass Balance Process Conditions and Product Summary — Sample 65	125
65	Hydrocarbon Distribution — Sample 65	126
66	Mass Balance Process Conditions and Product Summary — Sample 66	128
67	Slurry Screening Summary, $FeCo_3(CO)_{12}/K/Al_2O_3$ — 8385-60-707	129
	$\underline{FeCo_3(CO)_{12}/K/Al_2O_3}$ Mass Balance Results — 8385-60-707	
68	Mass Balance Process Conditions and Product Summary — Sample 3	130
69	Hydrocarbon Distribution — Sample 3	131
70	Mass Balance Process Conditions and Product Summary — Sample 6	133
71	Hydrocarbon Distribution — Sample 6	134
72	Mass Balance Process Conditions and Product Summary — Sample 8	136
73	Hydrocarbon Distribution — Sample 8	137
74	Mass Balance Process Conditions and Product Summary — Sample — 10	139
75	Hydrocarbon Distribution — Sample 10	140
76	Mass Balance Process Conditions and Product Summary — Sample 11	142
77	Hydrocarbon Distribution — Sample 11	143
78	Mass Balance Process Conditions and Product Summary — Sample 12	145
79	Hydrocarbon Distribution — Sample 12	146
80	Mass Balance Process Conditions and Product Summary — Sample 15	148

81	Hydrocarbon Distribution — Sample 15	149
82	Mass Balance Process Conditions and Product Summary — Sample 17	151
83	Hydrocarbon Distribution — Sample 17	152
84	Mass Balance Process Conditions and Product Summary — Sample 20	154
85	Hydrocarbon Distribution — Sample 20	155
86	Mass Balance Process Conditions and Product Summary — Sample 22	158
87	Hydrocarbon Distribution — Sample 22	159
88	Mass Balance Process Conditions and Product Summary — Sample 24	161
89	Hydrocarbon Distribution — Sample 24	162
90	Mass Balance Process Conditions and Product Summary — Sample 27	164
91	Hydrocarbon Distribution — Sample 27	165
92	Mass Balance Process Conditions and Product Summary — Sample 29	167
93	Hydrocarbon Distribution — Sample 29	168
94	Mass Balance Process Conditions and Product Summary — Sample 33	170
95	Hydrocarbon Distribution — Sample 33	171
96	Mass Balance Process Conditions and Product Summary — Sample 36	173
97	Hydrocarbon Distribution — Sample 36	174
98	Slurry Screening Summary, $Co_2(CO)_8/Zr(OPr)_4/Al_2O_3$ — 8523-1-4	175

$\underline{Co_2(CO)_8/Zr(OPr)_4/Al_2O_3}$ Mass Balance Results — 8523-1-4

99	Mass Balance Process Conditions and Product Summary — Sample 2	176
100	Hydrocarbon Distribution — Sample 2	177
101	Mass Balance Process Conditions and Product Summary —	179

	Sample 4	
102	Hydrocarbon Distribution — Sample 4	180
103	Mass Balance Process Conditions and Product Summary — Sample 7	182
104	Hydrocarbon Distribution — Sample 7	183
105	Mass Balance Process Conditions and Product Summary — Sample 10	185
106	Hydrocarbon Distribution — Sample 10	186
107	Mass Balance Process Conditions and Product Summary — Sample 13	188
108	Hydrocarbon Distribution — Sample 13	189
109	Mass Balance Process Conditions and Product Summary — Sample 17	191
110	Hydrocarbon Distribution — Sample 17	192
111	Mass Balance Process Conditions and Product Summary — Sample 20	194
112	Hydrocarbon Distribution — Sample 20	195
113	Mass Balance Process Conditions and Product Summary — Sample 25	197
114	Hydrocarbon Distribution — Sample 25	198
115	Mass Balance Process Conditions and Product Summary — Sample 29	200
116	Hydrocarbon Distribution — Sample 29	201
117	Mass Balance Process Conditions and Product Summary — Sample 32	203
118	Hydrocarbon Distribution — Sample 32	204
119	Mass Balance Process Conditions and Product Summary — Sample 34	206
120	Hydrocarbon Distribution — Sample 34	207
121	Mass Balance Process Conditions and Product Summary — Sample 38	209
122	Hydrocarbon Distribution — Sample 38	210
123	Mass Balance Process Conditions and Product Summary — Sample 40	212

124	Hydrocarbon Distribution — Sample 40	213
125	Mass Balance Process Conditions and Product Summary — Sample 43	215
126	Hydrocarbon Distribution — Sample 43	216
127	Mass Balance Process Conditions and Product Summary — Sample 47	218
128	Hydrocarbon Distribution — Sample 47	219
129	Mass Balance Process Conditions and Product Summary — Sample 50	221
130	Comparison of Cobalt Sources: $Co(NO_3)_2$ versus $Co_2(CO)_8$	222
131	Chemisorption Data for Supported Cobalt Catalysts	223

LIST OF FIGURES

FIGURE		PAGE
1	Co/Zr Weight Loading Ratio Effect on Specific Activity, $Co_2(CO)_8/Zr(OPr)_4/Al_2O_3$ Catalysts	224
	$Co_2(CO)_8/Ti(OPr)_4/Al_2O_3$ Mass Balance Results — 7888-1-589	
2	Hydrocarbon Weight Distribution — Sample 4	225
3	Hydrocarbon Weight Distribution — Sample 6	226
4	Hydrocarbon Weight Distribution — Sample 9	227
5	Hydrocarbon Weight Distribution — Sample 12	228
6	Hydrocarbon Weight Distribution — Sample 15	229
7	Hydrocarbon Weight Distribution — Sample 17	230
8	Hydrocarbon Weight Distribution — Sample 20	231
9	Hydrocarbon Weight Distribution — Sample 22	232
10	Hydrocarbon Weight Distribution — Sample 24	233
11	Hydrocarbon Weight Distribution — Sample 26	234
12	Hydrocarbon Weight Distribution — Sample 31	235
13	Hydrocarbon Weight Distribution — Sample 33	236
14	Hydrocarbon Weight Distribution — Sample 35	237
15	Hydrocarbon Weight Distribution — Sample 37	238
16	Hydrocarbon Weight Distribution — Sample 41	239
	$Co_2(CO)_8/Zr(OPr)_4/Al_2O_3$ Mass Balance Results — 7888-33-731	
17	Hydrocarbon Weight Distribution — Sample 8	240
18	Hydrocarbon Weight Distribution — Sample 10	241
19	Hydrocarbon Weight Distribution — Sample 12	242
20	Hydrocarbon Weight Distribution — Sample 16	243
21	Hydrocarbon Weight Distribution — Sample 21	244
22	Hydrocarbon Weight Distribution — Sample 24	245

23	Hydrocarbon Weight Distribution — Sample 28	246
24	Hydrocarbon Weight Distribution — Sample 33	247
25	Hydrocarbon Weight Distribution — Sample 36	248
26	Hydrocarbon Weight Distribution — Sample 39	249
27	Hydrocarbon Weight Distribution — Sample 44	250
28	Hydrocarbon Weight Distribution — Sample 47	251
29	Hydrocarbon Weight Distribution — Sample 52	252
30	Hydrocarbon Weight Distribution — Sample 65	253

$FeCo_3(CO)_{12}/K/Al_2O_3$ Mass Balance Results — 8385-60-707

31	Hydrocarbon Weight Distribution — Sample 3	254
32	Hydrocarbon Weight Distribution — Sample 6	255
33	Hydrocarbon Weight Distribution — Sample 8	256
34	Hydrocarbon Weight Distribution — Sample 10	257
35	Hydrocarbon Weight Distribution — Sample 11	258
36	Hydrocarbon Weight Distribution — Sample 12	259
37	Hydrocarbon Weight Distribution — Sample 15	260
38	Hydrocarbon Weight Distribution — Sample 17	261
39	Hydrocarbon Weight Distribution — Sample 20	262
40	Hydrocarbon Weight Distribution — Sample 22	263
41	Hydrocarbon Weight Distribution — Sample 24	264
42	Hydrocarbon Weight Distribution — Sample 27	265
43	Hydrocarbon Weight Distribution — Sample 29	266
44	Hydrocarbon Weight Distribution — Sample 33	267
45	Hydrocarbon Weight Distribution — Sample 36	268

$Co_2(CO)_8/Zr(OPr)_4/Al_2O_3$ Mass Balance Results — 8523-1-4

46	Hydrocarbon Weight Distribution — Sample 2	269
47	Hydrocarbon Weight Distribution — Sample 4	270
48	Hydrocarbon Weight Distribution — Sample 7	271
49	Hydrocarbon Weight Distribution — Sample 10	272

50	Hydrocarbon Weight Distribution — Sample 13	273
51	Hydrocarbon Weight Distribution — Sample 17	274
52	Hydrocarbon Weight Distribution — Sample 20	275
53	Bulk Activity versus Temperature at Various CO/H_2 Ratios and Space Velocities	276
54	Hydrocarbon Weight Distribution — Sample 25	277
55	Hydrocarbon Weight Distribution — Sample 29	278
56	Hydrocarbon Weight Distribution — Sample 32	279
57	Hydrocarbon Weight Distribution — Sample 34	280
58	Hydrocarbon Weight Distribution — Sample 38	281
59	Hydrocarbon Weight Distribution — Sample 40	282
60	Hydrocarbon Weight Distribution — Sample 43	283
61	Hydrocarbon Weight Distribution — Sample 47	284
62	Hydrocarbon Weight % Selectivity versus Reactor Temperature for Various CO/H_2 Ratios and Space Velocities	285
63	X-ray Photoelectron Spectra of Cobalt Catalysts	286

- CONTAINS POTENTIALLY PATENTABLE DATA — NOT FOR PUBLICATION -

1.0 INTRODUCTION

The future use of coal as a transportation fuel will depend on the development of an economical and energy efficient liquefaction process. The two most advanced processes are the direct liquefaction route involving the dissolution of coal in a solvent aided by a mild hydrogenation and the indirect route in which coal is first gasified to synthesis gas followed by the Fischer-Tropsch reaction. The indirect liquefaction process is the only one currently practiced commercially and, in this respect, has a firm data base of practical experience.

The Fischer-Tropsch reaction, in which carbon monoxide is reduced by hydrogen and polymerized, produces hydrocarbons with a broad range of molecular weights, from methane to paraffin waxes. This creates the need for further downstream processing such as hydrocracking and light olefin oligomerization to maximize the yield of liquid fuel product. Since the discovery of the Fischer-Tropsch reaction, extensive research has been aimed at controlling the product selectivity in order to minimize downstream refining and still remains a prime target for innovation. Previous research has shown that selectivity is mainly controlled by catalyst composition and process conditions. Despite the vast effort in catalyst research, no catalyst has been developed that yields a narrow product distribution of only gasoline or diesel fuel. Because of this, product selectivity has been more successfully controlled by manipulating process conditions.

Since the Fischer-Tropsch reaction is exothermic, control of the reaction heat plays a major role in determining product selectivity. Suspending the catalyst in a liquid medium offers the best means of heat transfer and temperature control. Thus slurry phase operation has been shown to give improved liquid product selectivity mainly by lowering the light gas yield. The amount of data from slurry phase operation, however, is limited to only a few studies and significant differences have been reported in yields, catalyst life and ease of operation. One consistent

observation is the lower gas yields and improved gasoline and diesel product selectivity. The improved temperature control has allowed this technology to be useful in converting carbon monoxide-rich synthesis gas from the latest coal gasifiers. Slurry phase operation also appears to be more amenable to scale-up. Much research remains to be done to fully determine the potential of slurry phase Fischer-Tropsch processing and its further development is an important part in our country's program to establish viable technology for converting coal to conventional hydrocarbon fuels.

Under prior contract number DE-AC22-80PC30021 with the Department of Energy, Air Products and Chemicals, Inc. developed several new slurry-phase Fischer-Tropsch catalyst systems that provided enhanced selectivity to liquid fuel products. One group of these catalysts was particularly novel in that it was prepared by supporting metal carbonyl clusters on alumina which had been modified by promoters. To further develop and improve these catalyst systems, Air Products, by the current contract to DOE, has begun a program to reproduce, evaluate and characterize these catalysts in detail. Examination of the catalyst kinetics in the slurry phase, along with fuel product characterization will be used to improve process design. Knowledge gained from these studies will provide a basis for the development of novel improved catalysts and process concepts for the selective production of liquid transportation fuels from synthesis gas. Work accomplished in the third quarter is described in this report.

- CONTAINS POTENTIALLY PATENTABLE DATA — NOT FOR PUBLICATION -

2.0 OBJECTIVE

The major goal of this project is to thoroughly investigate the preparation, characterization and performance of metal carbonyl cluster-based catalysts for use in slurry phase Fischer-Tropsch technology. As this understanding of catalyst behavior increases, improved catalysts will be designed and process concepts developed toward increasing catalyst activity, lifetime and selective production of liquid fuel product. The objectives will be addressed by the following four tasks:

Task 1 — Develop a project work plan which presents the detailed activities to be performed in achieving the objectives of this project. This task has been completed in the first quarter.

Task 2 — Develop improved supported cobalt and ruthenium carbonyl cluster-based catalysts by utilizing the promising leads discovered during prior work at Air Products under DOE contract number DE-AC22-80PC30021, which has shown that metal clusters supported on modified aluminas exhibit high activity, stability, and good selectivity to liquid fuels in the slurry phase Fischer-Tropsch process. New catalyst compositions designed to give enhanced selectivity to liquid fuels will also be developed.

In this task, catalysts will be evaluated and tested for their potential to convert synthesis gas into liquid hydrocarbon fuels. Catalysts will be studied by a combination of tests in stirred and fixed-bed reactors and will be evaluated on the basis of activity, selectivity, stability and aging. In addition, catalysts will be characterized by surface and bulk analyses.

Improvements in these catalysts will focus predominantly upon:

- Increasing catalyst activity

- Improving product selectivity for liquid fuels and reducing the yield of methane
- Developing catalyst systems active at high $CO:H_2$ ratios
- Incorporating water-gas shift activity, either directly in the catalyst or utilizing a mixture of catalysts in the slurry

Task 3 — The baseline catalyst compositions derived from both cobalt and ruthenium carbonyl clusters will be used to establish baseline slurry Fischer-Tropsch rate constants and activation energies. Then the more active and selective slurry catalyst compositions, identified under Task 2, will also be used in deriving slurry FT kinetic parameters. An existing backmixed CSTR model will be used in fitting the kinetic parameters. The kinetic parameters obtained will then be input to a three-phase bubble column computer model in order to predict conversions and space time yields in commercial scale bubble column units under a range of operating conditions.

An attempt will be made to determine kinetic expressions that describe the rate of formation of individual products or product fractions. This will be used to predict space time yields of individual product components or fuel fractions in a commercial scale bubble column.

Finally, mechanistic concepts will be examined, such as olefin reincorporation into growing chains, by adding small amounts of olefins to the feed and determining the effect on product selectivities.

Task 4 — In this task, hydrocarbon product fractions, accumulated from some of the longer slurry tests of the improved catalysts, will be collected under constant process conditions and subjected to a series of tests to evaluate their properties as specification fuel.

3.0 RESULTS AND DISCUSSION

3.1 Task 1 — Project Work Plan

This task was completed and reported on in the first quarter.

3.2 Task 2 — Development of Improved Supported Catalyst Compositions

(a) Catalyst Preparation

(i) $Co(NO_3)_2/Zr(OPr)_4/Al_2O_3$ (batch #8466-2)

A more conventional preparation of the $Co/Zr/Al_2O_3$ catalyst was examined by using $Co(NO_3)_2$ as the cobalt source in place of $Co_2(CO)_8$. The source of zirconium was still $Zr(OPr^n)_4$ but it was found that in solution (isopropanol) the material could be handled outside the dry box with insignificant hydrolysis. Catapal® SB Al_2O_3, heat treated in the standard fashion, was the support. After impregnating the alumina with $Zr(OPr)_4$/isopropanol solution, the material was air dried for 2 days then dried at 120°C for 3 hours. This was then impregnated to incipient wetness with aqueous $Co(NO_3)_2$, dried overnight at room temperature, then at 120°C for 1 hour and finally at 300°C for 6 hours, all in air. Elemental analysis of the resulting oxidized material gave the following results:

	Calculated	Found
Wt % Co	4.3	4.2
Wt % Zr	7.5	7.1
Co/Zr	0.57	0.59

(ii) $Co_2(CO)_8/Zr(OPr)_4/Al_2O_3$ (batch #8466-4)

A preparation of the basecase $Co/Zr/Al_2O_3$ composition was scaled up by 70% from the previous large scale preparation (batch # 7864-1010-371). This 366 g batch was the largest prepared to date and was made by the standard procedure. The composition obtained for this very large scale prep was quite comparable to that of the previous large scale basecase preparation as shown by the following elemental analysis:

	Batch 8466-4	Batch 7864-1010-371
Wt % Co	4.0	3.8
Wt % Zr	6.4	6.8
Co/Zr	0.63	0.56

This was further support for good reproducibility in the preparation of these catalysts both during scale-up and by different preparers.

(iii) $Co_2(CO)_8/Zr(OPr)_4/Al_2O_3$ (batch # 8466-9)

As part of the effort to examine the effect of metal loading on catalyst performance, a large batch (387 g) of $Co_2(CO)_8/Zr(OPr)_4/Al_2O_3$ catalyst was prepared using the standard procedure with an increased Co and Zr loading. The following metal loadings were obtained by elemental analysis:

	Calculated	Found
Wt % Co	10.0	10.8
Wt % Zr	8.4	8.5
Co/Zr	1.2	1.3

The Zr loading was not increased in the same proportion as the Co loading to facilitate the preparation of this high loading catalyst.

(b) Gas Phase Screening

All of the catalysts gas phase tested this quarter were activated using either the previously described syngas procedure (see October - December 1984 Quarterly Report) or a pure H_2 procedure as described in Section 4.1b. Specific run conditions did vary somewhat and are documented accordingly. Gas phase performance data is summarized in Table 1.

(i) $Co(NO_3)_2/Zr(OPr)_4/Al_2O_3$

Many carbonyl-derived catalysts had been tested during the first two quarters of this contract but no in-house reference point had been established for the conventional, cobalt nitrate-derived catalysts. This refererence point was determined this quarter by preparing and testing a $Co/Zr/Al_2O_3$ catalyst prepared from $Co(NO_3)_2$ in place of $Co_2(CO)_8$. Both syngas and pure H_2 activation procedures were examined for this catalyst and the results were as follows:

(a) Run # 7977-52-2, Batch # 8466-2

In this run, the cobalt nitrate-derived catalyst was activated by the syngas procedure from the fully oxidized state as it was initially charged to the reactor.

Testing was carried out at 240-280°C, 300 psig, 1:1 CO/H_2 and 1110 GHSV. Activity was minimal at 240°C and too little product was generated to obtain a mass balance. At 260°C, however, bulk activity was 23 mol syngas/kg

cat/hr with syngas conversion of 36%. This is slightly less active than the cobalt carbonyl derived catalysts running at 240°C. At 280°C, the bulk activity increased to 39 mol syngas/kg cat/hr with total CO + H_2 conversion of 59%. Although the activity may have been lower than the carbonyl catalyst, the selectivity was quite comparable and surprisingly was independent of run temperature.

(b) Run # 8413-1-2, Batch # 8466-2

A pure hydrogen activation was then examined on the same batch of cobalt nitrate-derived catalyst. Hydrogen at 3000 hr^{-1} GHSV and 0 psig was passed over the catalyst as it was heated to 300°C and maintained there for 16 hours. Subsequently, the temperature was reduced to the desired reaction temperature, carbon monoxide was introduced to give 1:1 CO/H_2 at 1000 GHSV and total pressure was increased to 300 psig.

The gas phase results showed that H_2 activition did improve the activity. In Table 130, the results obtained from the nitrate-derived catalyst using both activation procedures are compared with the results from a basecase carbonyl-derived composition activated with syngas.

Identical specific activity to the syngas-treated catalyst was achieved with the H_2-treated catalyst at 23° lower temperature. The H_2 activated catalyst even showed bulk activity of 9 mol syngas/kg cat/hr and 13% syngas conversion at 220°C. Using the standard syngas activation, no activity was observed even at 240°C. The cobalt carbonyl-derived catalyst activated with syngas, however, was still slightly more active than the

H_2-treated, cobalt nitrate-based catalyst at similar run conditions.

The nitrate-derived catalyst, activated by either procedure, showed increased wax selectivity which was as high as 20 wt% for the 240°C run. This may be due to larger cobalt particle sizes obtained by using $Co(NO_3)_2$, which is less reactive than $Co_2(CO)_8$ with the Al_2O_3 defect sites and, thus, not as prone to remain highly dispersed. The hydrocarbon distribution reflected a typical Schulz-Flory mechanism.

(ii) $\underline{Co_2(CO)_8/Zr(OPr)_4/Al_2O_3}$

A large batch (366 g) of the basecase $Co_2(CO)_8/Zr(OPr)_4/Al_2O_3$ composition was prepared to further confirm the reproducibility of the preparation procedure but more importantly to compare the standard syngas activation with pure H_2 activation. Hydrogen activation was done using neat H_2 at 0 psig, 300°C and 3000 hr^{-1} GHSV for 16 hours.

(a) Run # 8413-12-4, Batch # 8466-4

In this test, the catalyst was activated with syngas in the standard fashion. The performance was similar to previous $Co_2(CO)_8$-based catalysts. At 240°C, CO/H_2 = 1.0 and 1000 hr^{-1} GHSV, the bulk activity was average at 21 mols syngas/kg cat/hr with a syngas conversion of 48%. Specific activity appeared somewhat low at 0.16 mols CO/mol Co/min. Liquid fuel (C_5-C_{23}) selectivity was also typical at 60 wt%. All the results, including those at 220°C and 260°C, are summarized in Table 1.

(b) Run # 8413-20-4, Batch # 8466-4

A charge of fresh catalyst from the same batch was then tested after activating with pure H_2 as described above. Hydrogen activation resulted in higher activity, especially at lower run temperatures (220° and 240°). At 260°C, the difference was minimal and slightly higher conversions were observed for the syngas activated catalyst but this was probably a result of the lower space velocity used for this test. At 220°C, both bulk and specific activity more than doubled. At 240°C, the increase in activity was less but still significant at 27%. There was no significant difference in hydrocarbon selectivity between the two activation procedures.

(c) Slurry Phase Testing

Four catalysts were tested in the 1 liter slurry phase reactors this quarter. In each case, a series of operating conditions was investigated to determine the optimum for activity and hydrocarbon selectivity. The following three catalysts were tested following the standard synthesis gas activation method conducted in the tubular gas phase reactor:

- titanium promoted $Co_2(CO)_8$ on alumina in place of the zirconium promoter
- zirconium promoted $Co_2(CO)_8$ on alumina with a metals ratio, Co/Zr, of 1.15 to compare with the standard ratio of 0.56.
- $FeCo_3(CO)_{12}$ on alumina promoted with potassium.

A fourth catalyst, $Co_2(CO)_8$ on zirconated alumina, with approximately the standard Co/Zr weight ratio of 0.65 was activated

with H_2 for comparison to synthesis gas activation. Representative data from these tests along with previous test results of the catalysts tested in quarters 1 and 2 are summarized in Table 2. The details of each of this quarter's catalyst tests are given below.

(i) $Co_2(CO)_8/Ti(OPr)_4/Al_2O_3$ - 7888-1-589

The test of $Co_2(CO)_8$ on alumina promoted with titanium was completed this quarter. The major objective of this test was to determine the effect of titanium as promoter on activity and hydrocarbon selectivity. The details of the preparation and activation are given in section 4.1.

The activity, conversion and selectivity data of the major sample points are summarized in Table 3. The individual mass balances of this screening test are listed in Tables 4-33 and illustrated in Figures 2-41.

The first five mass balances were conducted at 240°C, with variations in the CO/H_2 ratio of 1.0 to 2.0, space velocities of 0.9 and 1.8 NL/g cat/hr, and pressures of 300 and 600 psig. The test was initiated at CO/H_2 = 0.98, 300 psig and 1.8 NL/g cat/hr (sample 4, Tables 4-5, Figure 2). The bulk activity of 24.9 mol syngas/kg cat/hr was comparable to the zirconated catalyst activity (Run #7595-60-C48.4). The specific activity, however, was low at 0.22 mols CO/mol Co/min compared with, for example, the $Ru_3(CO)_{12}$ on zirconated alumina (Run # 7887-36-478). The selectivity for liquid fuels, C_5-C_{23}, was high at 63.8 wt% of the total hydrocarbons.

The CO/H_2 ratio was next raised to 1.5 in an attempt to shift the lighter products into the heavier molecular weight region (sample 6, Tables 6-7, Figure 3). The results were promising with an increase in the C_5-C_{23} selectivity to 68.1

wt%, but with a nearly 40% decrease in bulk activity to 17.7 mol syngas/kg cat/hr. The activity further fell to 13.7 mol syngas/kg cat/hr at CO/H_2 = 2.0 with no apparent improvement in fuels selectivity (sample 9, Tables 8-9, Figure 4). The corresponding decrease in specific activity to 0.14 mols CO/mol Co/min indicates poor water-gas shift activity at high CO/H_2 feed ratios.

The space velocity was then lowered to 0.9 NL/g cat/hr maintaining the CO/H_2 at 2.0, and pressure at 300 psig (sample 12, Tables 10-11, Figure 5). The effect on the hydrocarbon selectivity was negligible. The overall conversion increased by 43% with equivalent increases in the H_2 and CO conversions. The usage ratio continued to be poor at 0.6.

The operating pressure was next raised to 600 psig and the CO/H_2 ratio lowered to 1.6 (sample 15, Tables 12-13, Figure 6). A substantial increase in methane selectivity to 11.3 wt% occurred with a corresponding decrease in fuels selectivity. A 23% decrease in overall conversion was also observed.

The next five test conditions were conducted at 260°C. At CO/H_2 = 2.0, 0.9 NL/g cat/hr, and 300 psig (sample 17, Tables 14-15, Figure 7) a 16% increase in activity to 11.1 mol syngas/kg cat/hr over sample 12 at 240°C (other operating conditions the same) was observed. The selectivity to liquid fuels, C_5-C_{23}, returned to the 65 wt% level of sample 12, but with still a high methane selectivity.

The space velocity was next raised to 1.81 NL/g cat/hr (sample 20, Tables 16-17, Figure 8). Compared with the lower temperature results at the same CO/H_2 ratio, space velocity, and total pressure, the bulk activity was 17% higher at 16.0 mol syngas/kg cat/hr, with the same total fuels selectivity of

65 wt%. The increase in methane selectivity to 13 wt% from 8 wt% indicates a redistribution of products to the lighter molecular weight region with increasing temperature.

At 1.81 NL/g cat/hr, the CO/H_2 ratio was next lowered to 1.5 (sample 22, Tables 18-19, Figure 9). The bulk activity increased to 17.8 mol syngas/kg cat/hr with a slight increase in methane selectivity to 14.5 wt%. In general, the overall hydrocarbon distribution did not change. The effect of doubling the pressure to 600 psig was tested next.

At 258°C, CO/H_2 = 1.4, 600 psig and 1.87 NL/g cat/hr (sample 24, Tables 20-21, Figure 10), the bulk activity was 23% higher than at the similar conditions at 300 psig. The fuels yield fell to 61 from 65 wt% with a redistribution of products into the lighter molecular weight region. An attempt at enhancing chain propagation by reducing the space velocity to 0.96 NL/g cat/hr failed (sample 26, Tables 22-23, Figure 11). The increase in methanation activity continued with a corresponding reduction in fuels selectivity.

During the next three mass balance days, the temperature was maintained at 280°C (samples 31, 33, and 35, Tables 24-29, Figures 12-14). At this point it was obvious that the catalyst had deactivated since activities lower than at 260°C were observed. This was further confirmed when two operating points from the beginning of the run were repeated to check for reproducibility (samples 37 and 41, Tables 30-33, Figures 15-16). Sample 37 was 50% less active than sample 20, and sample 41 was 117% less active than sample 9. The methane selectivity was 16 wt% and 22 wt%, respectively.

(ii) $Co_2(CO)_8/Zr(OPr)_4/Al_2O_3$ - 7888-33-731

The screening test of $Co_2(CO)_8$ on zirconated alumina with a metals loading of 5.07% Co and 4.39% Zr (preactivated) was completed this quarter. The major objective of this test was to determine the effect of the Co/Zr weight ratio loading on catalyst activity and selectivity. The following three tests, with varying Co/Zr ratios were then comparable:

Run No.	Wt% Co	Wt% Zr	Co/Zr
7595-60-C48.4	3.81	6.84	0.56
7887-67-445	4.71	0	
7888-33-731	5.07	4.39	1.15

The synthesis gas activation method used and the details of the catalyst preparation are included in Section 4.1. The activity, conversion and selectivity data of the major sample points are summarized in Table 34. The individual mass balances are listed in Tables 35-66 and illustrated in Figures 17-30.

The test was initiated at 240°C with the following four CO/H_2 feed ratios and space velocity changes:

Sample	CO/H_2	NL/g cat/hr
8	1.01	1.76
10	1.69	1.69
12	2.00	1.72
16	1.95	0.86

The highest liquid fuels selectivity of 70 wt% C_5-C_{23} was obtained at the sample 8 conditions (Tables 35-36, Figure 17). The bulk activity, however, was only mediocre at 15.3 mols syngas/kg cat/hr. The CO/H_2 ratio was increased to reduce

methanation activity (samples 10 and 12, Tables 37-40, Figures 18 and 19). The major result was a threefold increase in wax selectivity to 12.6 wt% $C_{24}+$, with only a 26% reduction in methane selectivity to 8.8 wt%. This trend was accompanied by a gradual decrease in bulk activity to 8.7 mol syngas/kg cat/hr.

The shifting of products to the heavier molecular weight region continued at a lower space velocity of 0.86 NL/g cat/hr (sample 16, Tables 41-42, Figure 20). An approximately 4% reduction in liquid fuels selectivity was observed. The overall conversion was 16% lower than expected upon halving the space velocity. The usage ratio showed no improvement in water-gas shift activity with values in the 0.3-0.5 range for the above feed ratios.

The following six process conditions were next tested at 260°C:

Sample	CO/H_2	NL/g cat/hr
21	1.94	0.86
24	0.98	0.86
28	0.98	1.73
33	1.46	1.73
36	0.98	1.41
39	0.98	0.71

A 65% increase in bulk activity to 12.4 mols syngas/kg cat/hr was obtained at the sample 21 conditions as a result of the 20°C increase in temperature (Tables 43-44, Figure 21). No appreciable change in hydrocarbon selectivity was observed. At the same space velocity, the CO/H_2 ratio was next reduced to 0.98 (sample 24, Tables 45-46, Figure 22). A 35% increase in

bulk activity accompanied but a 75% increase in methane selectivity was observed.

The space velocity was next returned to 1.73 NL/g cat/hr (sample 28, Tables 47-48, Figure 23). An 80% increase in bulk activity was observed with a specific activity of 0.16 mol CO/mol Co/min. The change in hydrocarbon distribution was negligible compared with sample 24.

The CO/H_2 ratio was next increased to 1.46 to try to reduce methanation activity (sample 33, Tables 49-50, Figure 24). The selectivity to liquid fuels returned to the high 68 wt% observed previously, but the methane selectivity remained high at 14.9 wt%. Because of poor water-gas shift activity, the bulk activity fell dramatically by 35% to 20.1 mol syngas/kg cat/hr.

The results of samples 36 and 39 (Tables 51-54, Figures 25-26) were good indicators of the effect of space velocity on product selectivity. At a space velocity of 1.41 NL/g cat/hr the methane selectivity was 16.6 wt% and the wax selectivity was 8.0 wt%. When the space velocity was halved, a definite trend toward shifting products to the heavier molecular weight region was observed. The wax selectivity nearly doubled to 15.6 wt%. It is worth noting that the bulk activity was half that of sample 36, 12.7 mol syngas/kg cat/hr. No appreciable deactivation was apparent at this point.

The next set of conditions which were investigated were at 280°C:

Sample	CO/H_2	NL/g cat/hr
44	0.96	0.71
47	1.94	0.70
52	1.95	1.40

A 10% increase in activity was observed for sample 44 (Tables 55-56, Figure 27). This was accompanied by a 76% increase in methane selectivity and a corresponding decline in liquid fuels selectivity to 49.1 wt%. Increasing the CO/H_2 ratio to 1.95 improved liquid fuels selectivity by 10% to 54 wt% (sample 47, Tables 57-58, Figure 28), but this was substantially lower than the 70 wt% selectivity observed at the initial conditions at 240°C. When the space velocity was next raised to 1.40 NL/g cat/hr, an 8% increase in fuels selectivity was observed (sample 52, Tables 59-60, Figure 29), but at the expense of a 24.4 wt% methane selectivity. Only a 44% increase in bulk activity resulted upon doubling the space velocity. The remainder of this test was devoted to determining the effect of ethylene addition on hydrocarbon selectivity.

(iii) $FeCo_3(CO)_{12}/K/Al_2O_3$ - 8385-60-707

The screening test of the Al_2O_3 supported $FeCo_3(CO)_{12}$ cluster promoted with K with a metals loading of 0.78% Fe: 2.44% Co: 0.02% K (preactivated) was completed. The major objective of this test was to determine if the K promoted, mixed Fe/Co cluster catalyst has any advantage in either activity or selectivity over the unpromoted Fe/Co catalyst tested previously (Run # 8385-22-677).

The synthesis gas activation method was the same as that used for the above two catalysts. This, along with the details of the preparation, are presented in Section 4.1. The activity, conversion and selectivity data of the major sample

points of this screening test are summarized in Table 67. The individual mass balances are listed in Tables 68-94 and illustrated in Figures 31-45.

The test was initiated at 240°C with the following four CO/H_2 feed ratio and space velocity changes:

Sample	CO/H_2	NL/g cat/hr
3	1.01	1.6
6	1.52	1.6
8	2.01	1.6
10	2.02	0.7

The general trend during these first three test conditons (samples 3,6 and 8, Tables 68-73, Figures 31-33) was a decrease in activity with increasing CO/H_2 ratio and increase in the selectivity of liquid fuels from 58.0 to 62.8 wt%. The selectivity to methane, as expected, showed a similar trend, i.e., a reduction from 14.0 to 9.8 wt%. When the space velocity was reduced to 0.7 NL/g cat/hr for sample 10 (Tables 74-75, Figure 34), the products shifted to the heavier molecular weight region, but with a reduction in liquid fuels selectivity to 62.7 wt%. The next five test conditions were conducted at 260°C:

Sample	CO/H_2	NL/g cat/hr
11	2.02	0.7
12	2.03	1.6
15	1.52	1.6
17	1.01	1.5
20	1.00	0.7

Sample 11, at the same CO/H_2 ratio and space velocity as sample 10, showed an 86% increase in activity (Tables 76-77,

Figure 35). The 11% increase in fuels selectivity to 69.3% was a result of the shift in wax products into this range. This general trend continued when the space velocity was raised to 1.6 NL/g cat/hr (sample 12, Tables 78-79, Figure 36). At these conditions, the fuels yield was the highest at over 70 wt%, comparable only to that of $Ru_3(CO)_{12}/Zr/Al_2O_3$ (Run # 7887-36-478).

As the CO/H_2 ratio was reduced to 1.5 and then to 1.0 in the next two samples 15 and 17 (Tables 80-83, Figures 37-38), the selectivity to methane increased from 10.0 to 16.7 wt%. When the space velocity was next reduced to 0.7 NL/g cat/hr, the fuels selectivity increased once more to 66.2 wt% (sample 20, Tables 84-85, Figure 39).

The following five operating conditions were conducted at 280°C:

Sample	CO/H_2	NL/g cat/hr
22	1.00	0.7
24	2.02	0.7
27	1.01	1.5
29	2.03	1.5
33*	1.96	1.5

*625 psig

A 37% increase in bulk activity to 19.1 mol syngas/kg cat/hr was obtained for sample 22 (Tables 86-87, Figure 40). A slight shift in product distribution produced a methane selectivity of 15.3 wt%, but with no appreciable change in the fuels selectivity compared with sample 20 at 260°C. When the CO/H_2 ratio was raised to 2.02 (sample 24, Tables 88-89, Figure 41), a 5% increase in fuels selectivity to 70.1 wt% was

observed. Unfortunately, a drastic 67% reduction in activity was also the result.

In the next two samples the space velocity was raised to 1.5 NL/g cat/hr (samples 27 and 29, Tables 90-93, Figures 42-43). Once again, the effect of the CO/H_2 ratio on activity and selectivity was observed. At CO/H_2 = 1.01, the methane selectivity was 19.1 wt% and the activity 27.3 mol syngas/kg cat/hr. When the ratio was raised to 2.03, both the activity and methane selectivity fell to 17.5 mol syngas/kg cat/hr and 13.9 wt%, respectively. The selectivity to fuels improved to 64.7% with an increase in the CO/H_2 ratio, but not to the level observed at 260°C.

To determine the effect of high pressure operation, the total system pressure was raised to 625 psig (sample 33, Tables 94-95, Figure 44). A 43% reduction in activity was observed and a 7% reduction in total fuels selectivity. This again verified the negative effect of high pressure operation on both the activity and selectivity of these catalysts.

For a final check on catalyst performance, the process conditions were returned to 240°C, CO/H_2 = 1.0 and 1.5 NL/g cat/hr (sample 36, Tables 96-97, Figure 45). The activity was 4.1 compared with the original 11.3 mol syngas/kg cat/hr of sample 3. This was probably due to the operation at 625 psig.

(iv) <u>$Co_2(CO)_8/Zr(OPr)_4/Al_2O_3$ - 8523-1-4</u>

The objective of this test was to try to improve catalyst activity by using a H_2 reduction instead of the usual synthesis gas activation procedure. The metals loadings of this catalyst, 5.06 wt% Co and 7.82 wt% Zr, was similar to that of the basecase catalyst (Run # 7595-60-C48.4).

A description of the activation and method of preparation are detailed in Section 4.1. The activity, conversion and selectivity data of the major sample points of this screening test are summarized in Table 98. The individual mass balances are listed in Tables 99-129 and illustrated in Figures 46-62.

Process conditions at a lower than usual temperature level of 220°C were tested initially due to the high activity observed in the gas phase test:

Sample	CO/H_2	NL/g cat/hr
2	1.00	1.85
4	1.48	1.86
7	1.43	0.95

As suspected, even at 220°C, it was apparent that the hydrogen activation method improved catalyst activity dramatically. Compared with similar test conditions from the basecase catalyst (7595-60-C48.4), the bulk activity of sample 2 (Tables 99-100, Figure 46) was 80% higher. Also, the methane selectivity was 28% lower at 10.6 wt% and the total liquid fuels selectivity was 13% greater at 62.1 wt%. With an increase in the CO/H_2 ratio and reduction in space velocity (sample 4 and 7, Tables 101-104, Figures 47-48), the trend was to decreased activity and methane selectivity and increased liquid fuels yield.

The following four process conditions tested were next conducted at 240°C:

Sample	CO/H_2	NL/g cat/hr
10	1.43	0.95
13	1.88	0.94

17	1.99	1.87
20	0.99	1.86

A 38% increase in activity was observed for sample 10 (Tables 105-106, Figure 49). Interestingly, the liquid fuels selectivity increased from 64.0 to 67.2 wt% with a reduction in methane selectivity to 7.8 wt%. The CO/H_2 ratio was then raised to 1.88 (sample 13, Tables 107-108, Figure 50). The major effect was the reduction in wax selectivity, $C_{24}+$, to 8.3 wt% from 11.7 wt%. The next two samples, at double the space velocity (samples 17 and 20, Tables 109-112, Figures 51-52), further verified the trends which were observed with the synthesis gas activated catalysts, but appeared to be more pronounced when the H_2 activation method was used. Figure 53 illustrates this trend in decreasing bulk activity with the CO/H_2 ratio at the two space velocities studied. The maximum fuels selectivity obtained at 240°C was high at 69.3 wt%.

The performance of this catalyst was next investigated at 260°C at the following conditions:

Sample	CO/H_2	NL/g cat/hr
25	0.99	1.86
29	1.48	1.87
32	1.44	0.95
34	1.87	0.94

Once again, at the lowest CO/H_2 ratio, the bulk activity was considerable at 38.5 mol syngas/kg cat/hr (sample 25, Tables 113-114, Figure 54). The specific activity was the highest, 0.32 mol CO/mol Co/min, of the Co based catalysts tested to date. The $Ru_3(CO)_{12}$ catalyst tested in the last quarter (Run # 7887-36-478) had better specific activity, but not bulk activity. The hydrocarbon distribution was more in

favor of fuels production with over 70 wt% selectivity. The three remaining samples at 260°C followed a similar trend in bulk activity with space velocity and CO/H_2 ratio changes as at the provious two temperatures studied as shown in Figure 53 (samples 29-34, Tables 115-120, Figures 55-57).

Finally, the temperature was raised to 280°C for tests at the following conditons:

Sample	CO/H_2	NL/g cat/hr
38	1.88	0.94
40	1.43	0.95
43	1.48	1.86
47	1.95	1.85

The data followed the expected trend in bulk activity, but this increase was not as pronounced as during previous temperature increases (samples 38-47, Tables 121-128, Figures 58-61). The trend in selectivity is well illustrated in Figure 62; the selectivity to liquid fuels was optimum at 260°C, irrespective of the CO/H_2 ratio or space velocity.

A check of reproducibility of the results of the initial test conditions was attempted (sample 50, Table 129). The accuracy of this sample, however, was suspect since the product selectivity was not uniform. Gaps in the C_6-C_{10} region were substantial indicating bad sampling. The bulk activity was 3.8 compared with 23.6 mol syngas/kg cat/hr of sample 2.

(d) Catalyst Characterization

Preliminary XPS data have been obtained on the large batch of basecase $Co_2(CO)_8/Zr(OPr)_4/Al_2O_3$ catalyst (batch #8466-4) as freshly prepared and after H_2 activation. XPS analysis has also been

performed on the oxidized, cobalt nitrate-derived $Co/Zr(OPr)_4/Al_2O_3$ composition (batch # 8466-2). The carbonyl derived catalyst exhibits binding energies corresponding to complete oxidation of Co^0 to Co^{2+} due to reaction of the carbonyl with the alumina or zirconium. This agrees with the published literature. This Co^{2+} remains oxidized after H_2 activation and may be due to formation of non-reducible cobalt aluminates or zirconates at the elevated activation temperature. The nitrate derived material shows binding energies for Co^{2+} and Co^{3+} indicating the presence of $CoAl_2O_3$ and Co_3O_4. The XPS spectra are shown in Figure 63.

B.E.T. surface area and hydrogen chemisorption data have been obtained for the three catalysts prepared this quarter. The data are summarized in Table 131. Total surface area of the fresh catalysts changed very little from that of the support (217 m^2/g for Catapal® SB γ-alumina after calcining at 500°C for 3 hours). Hydrogen chemisorption showed the metal surface areas and dispersions to be quite low. There was no difference in hydrogen chemisorption between the cobalt carbonyl and cobalt nitrate catalysts, but the cobalt carbonyl catalyst with a higher Co loading showed slightly larger metal surface area and dispersion. This was opposite of what would be expected, that is as metal loading increases dispersion should decrease. The H_2 chemisorption also appeared to be activated since hydrogen uptake increased with temperature. This phenomenum has been observed by others and reported in the literature. The observed H_2 chemisorption behavior suggests a strong interaction with the support or an overlayer effect. The chemisorption results are in agreement with the XPS data showing that only small amounts of cobalt were reduced.

3.3 Task 3 — Slurry Reactor Kinetic Studies

Mechanistic concepts were examined this quarter by studying the effects of adding ethylene to the feed. It has been postulated that light olefins, produced in the F-T synthesis, may be reincorporated into the surface carbon chain growth process, thus allowing for variations in selectivity. These experiments were performed at the end of the screening test of the $Co_2(CO)_8/Zr(OPr)_4/Al_2O_3$ catalyst (Run # 7888-33-731), by adding 10 and 20 volume percent ethylene to the feed. The following four test condition were conducted at 260°C:

Sample	P, psig	$CO/H_2/C_2H_4$ vol%	NL/g cat/hr
56	308	44/46/10	1.41
59	302	39/41/20	1.41
62	300	40/40/20	0.71
65	300	51/43/0	0.70
66	550	40/40/20	1.40

The major result of adding 10 and 20 volume percent ethylene during samples 56, 59 and 62 (Tables 61-63) was the production of ethane. The rates of oxygenate production also increased, from 0.2 to 2.4 wt% of the total product yield, but with the majority of this fraction being propanol. No evidence of olefin reincorporation was observed.

The process conditions were next returned to that of sample 39, CO/H_2 = 0.98, 0.7 NL/g cat/hr, to determine the extent of catalyst deactivation before the high pressure operation with ethylene addition was investigated (sample 65, Tables 64-65, Figure 30). A 40% reduction in bulk activity was observed with methane selectivity at over 20 wt% compared with the 14.3 wt% of sample 39. Once more, the major product with ethylene addition and 550 psig was ethane (sample 66, Table 66). A 23% increase in gasoline fuels, C_5-C_{11}, was observed, but this was due mainly to a general shift in products into the heavier molecular weight region which is

expected at high pressure. Compared with sample 59, the oxygenates selectivity increased from 1.49 to 2.06 wt%., again with mainly propanol production.

4.0 EXPERIMENTAL

4.1 Task 2 — Development of Improved Supported Catalyst Compositions

(a) Catalyst Preparation

The catalysts prepared this quarter all had calcined γ - alumina as the support. Calcination and handling procedures were described in the first quarterly report.

(i) $Co(NO_3)_2/Zr(OPr)_4/Al_2O_3$ (Batch # 8466-2)

To establish a reference catalyst, a more conventional preparation of the $Co/Zr/Al_2O_3$ composition was examined by using $Co(NO_3)_2$ as the cobalt source in place of $Co_2(CO)_8$. Zirconium propoxide was still used but it was found that in solution the material could be handled in the ambient lab atmosphere without noticeable hydrolysis. A solution (210 cc total volume) of 59.6 g of $Zr(OPr)_4$ in isopropanol was added to 174.2 g of calcined Catapal® SB γ-alumina in two portions with thorough mixing to give incipient wetness. The impregnated alumina was allowed to dry in ambient air for two days and then for three hours at 120°C in air. Cobalt nitrate (44.1 g) was dissolved in deionized water to give 200 cc of solution which was impregnated into the zirconated alumina in one portion. This material was allowed to dry overnight at room temperature then at 120°C for one hour and was finally calcined in air at 300°C for six hours to give 211 g of catalyst. Elemental analysis of this material gave 4.2% Co and 7.1% Zr (Co/Zr weight ratio = 0.59).

(ii) $Co_2(CO)_8/Zr(OPr)_4/Al_2O_3$

(a) Batch # 8466-4

This batch was a 70% scale-up of the previous large scale preparation of the basecase (batch # 7864-1010-371) $Co/Zr/Al_2O_3$ composition. Standard inert atmosphere handling techniques were used in preparing this catalyst; exposure to oxygen and moisture was prevented throughout this preparation. 250 g of alumina was impregnated in one portion with a 300 cc solution of $Zr(OPr)_4$, 84.2 g, in hexane. After mixing thoroughly by shaking the flask, the hexane was evaporated off in vacuo with slight warming in a 40-50°C bath. To load the cobalt, a two step addition of 40.0 g of $Co_2(CO)_8$ in hexane was used. The first portion was a 350 cc volume followed by a 300 cc second portion. After each portion hexane was removed in vacuo as before. After complete removal of the solvent, 366 g of brownish-black catalyst was obtained and analyzed as 4.0% Co and 6.4% Zr (Co/Zr weight ratio = 0.63).

(b) Batch # 8466-9

To examine the effect of metal loading on catalyst performance some $Co/Zr/Al_2O_3$ catalyst was prepared with an increased Co and Zr loading using the standard impregnation procedure. $Zr(OPr)_4$, 127.5 g, was dissolved in hexane to give 210 cc of solution, which was mixed with 172.5 g of alumina in the dry box. The sealed flask containing the impregnated alumina was removed from the dry box so that the solvent could be evaporated off on the vacuum line. Half of the 123.4 g of $Co_2(CO)_8$ was dissolved in 300 cc of 1:1 hexane/toluene and added to the zirconated alumina. After solvent removal, the remaining

$Co_2(CO)_8$, dissolved in 250 cc of toluene, was added. The dried, black catalyst weighed 387 g and was analyzed as 10.8 % Co and 8.5% Zr (Co/Zr weight ratio = 1.3).

(b) Gas Phase Screening

A detailed description of the gas phase screening reactor and procedure can be found in the Project Work Plan. The catalyst charge was 10 cc for each test. Generally, only reactor temperature and CO to H_2 feed ratio were varied while pressure and space velocity were kept at 300 psig and 1000 h^{-1} (v/v), respectively, for all the runs. The syngas activation procedure has been described previously in the first quarter report. For two of this quarter's tests, a pure H_2 activation was used as follows: Hydrogen at 3000 hr^{-1} and 0 psig was passed over the catalyst as it was heated to 300°C at 3°/min and maintained there for 16 hours. The temperature was then reduced to the desired reaction temperature, CO was introduced to give 1:1 CO/H_2 at 1000 hr^{-1} and finally the total pressure was increased to 300 psig.

(c) Slurry Phase Tests

(i) $Co_2(CO)_8/Ti(OPr)_4/Al_2O_3$ - 7888-1-589

This catalyst was activated in the gas phase reactor using a 20% 1:1 CO/H_2 in N_2 at 175 psig and 500 hr^{-1} GHSV. The temperature was raised in 10°C stages from 220 to 280°C. After cooling under N_2, the activated catalsyt was slurried in deoxygenated Fischer paraffin oil (catalog # 0-122) and transferred to the reactor under a N_2 atmosphere. The final loading was 408 mls of a 22.3 wt% slurry containing 91.1 gms of activated catalyst. The elemental analysis before activation was:

	Wt%
Co	3.49
Ti	8.65

(ii) $Co_2(CO)_8/Zr(OPr)_4/Al_2O_3$ - 7888-33-731

This catalyst was activated and slurried in the same manner as the catalyst above. The final reactor loading was 452 mls of a 23.4 wt% slurry containing 96.0 gms of activated catalyst. The elemental analysis prior to activation was:

	Wt%
Co	5.07
Zr	4.39

(iii) $FeCo_3(CO)_{12}/K/Al_2O_3$ - 8385-60-707

This catalyst was activated and slurried in the same manner as described above. The final reactor loading was 444 mls of a 20.6 wt% slurry containing 88.1 gms of activated catalyst. The elemental analysis before activation was:

	Wt%
Fe	0.78
Co	2.44
K	0.02

(iv) $Co_2CO)_8/Zr(OPr)_4/Al_2O_3$ - 8523-1-4

This catalyst was gas phase activated using H_2. The fresh catalyst, 107.5 gms, was loaded into the 150 cc tubular reactor (approximately 110 cc catalyst bed volume). The reactor was heated at ambient pressure to 300°C at a rate of 1°C/min and a space velocity of 0.56 NL/g cat/hr H_2. The temperature was

maintained at 300°C for 15 hours with full H_2 flow. After cooling under N_2, the activated catalyst was slurried in deoxygenated Fischer paraffin oil and transferred to the reactor under a N_2 atmosphere. The final loading was 470 mls of a 16.9 wt% slurry containing 75.96 gms of activated catalyst. The elemental analysis after activation was:

	Wt%
Cc	5.06
Zr	7.82

(d) Catalyst Characterization

XPS data was obtained on a Physical Electronics 560 XPS/AES instrument. Catalyst samples were reduced in the 10 cc fixed bed reactor and transferred to the sample holder in a dry box. H_2 chemisorption experiments were conducted on a Micromeritics Chemisorb 2800 using catalyst samples prereduced in the 10 cc reactor. After transfer of the samples to the chemisorption sample tubes, they were treated with H_2 at 300°C and 1 atmosphere prior to data aquisition. B.E.T. surface areas were obtained using a Micromeritics Digisorb 2500.

5.0 ACKNOWLEDGEMENTS

The skilled technical assistance of P. A. Dotta, G. W. Long, M. Louie and L. E. Schaffer is gratefully acknowledged.